

## Energy Levels in $\text{Pb}^{206}$ from the Decay of $\text{Bi}^{206}$

D. E. ALBURGER,\*

*Nobel Institute of Physics, Stockholm, Sweden, and Brookhaven National Laboratory,† Upton, New York*

AND

M. H. L. PRYCE, *Clarendon Laboratory, Oxford, England*

(Received June 14, 1954)

The energies, spins, and parities of 10 excited states in  $\text{Pb}^{206}$  and the probable energies, spins, and parities of two additional states have been established by studies of 6.4-day  $\text{Bi}^{206}$  decay. The experiments include—intensity and precision energy measurements on the conversion lines in a double-focusing spectrometer; coincidences between pairs of  $K$ -conversion lines in a two-lens “spectrogoniometer”; coincidences between gamma rays and conversion electrons in a modified intermediate-image spectrometer; discovery of a  $145 \pm 15$  microsecond isomeric state decaying by either of two  $E3$  transitions; examination of the low-energy conversion spectrum; and relative gamma intensity measurements with a scintillation spectrometer. The adopted decay scheme contains 28 of the observed transitions and satisfies all of the conditions imposed by the energy and coincidence measurements. A few additional very weak transitions are unassigned. It is shown from a theoretical analysis based on the shell model that the observed levels are in agreement with the approximate calculations. Eleven gamma rays decaying with a half-life of 14 days are assigned to  $\text{Bi}^{206}$ .

### I. INTRODUCTION

THE nucleus  $\text{Pb}^{206}$  differs from the double closed-shell  $\text{Pb}^{208}$  by two neutrons, and its level structure should thus be largely predictable<sup>1</sup> in terms of the shell model. It is a stable nucleus, which also occurs as the end point of three known radioactivities. Of these, the beta decay of  $\text{Tl}^{206}$  leads always to the ground state<sup>2</sup> so that no information concerning the level structure of  $\text{Pb}^{206}$  is obtained. The alpha decay of  $\text{Po}^{210}$  goes mainly to the ground state, but in a small fraction of the disintegrations leaves the  $\text{Pb}^{206}$  nucleus in its first excited state at 803 keV. The other activity is the 6.4-day electron capture of  $\text{Bi}^{206}$  which leaves the  $\text{Pb}^{206}$  in a highly excited state and is followed by a complex spectrum of gamma rays. Alburger and Friedlander<sup>3</sup> found fifteen gamma rays in  $\text{Bi}^{206}$  decay, including one whose energy agreed with the 803-keV radiation in the decay of  $\text{Po}^{210}$ .

Evidence on the excited levels of  $\text{Pb}^{206}$  can also be derived<sup>4</sup> from the reaction  $\text{Pb}^{207}(d,t)\text{Pb}^{206}$ , which indicates levels at 0.86, 1.37, 1.71, 2.22, and 3.03 MeV, but these are probably unresolved groups of levels.

The present paper reports a continuation of the investigation of the spectrum of  $\text{Bi}^{206}$ , using more precise and powerful techniques, in the course of which twenty-eight gamma rays have been established, all of which can be fitted into a term diagram, together with a number of radiations of very low energy whose precise interpretation is still uncertain. Except for four gamma rays and two energy levels, the assignment of energies, spins, and parities of the levels, and

multipole character of the gamma rays, can be regarded as reasonably unambiguous. Twelve excited levels are involved in all, of which one (at 2200.3 keV, spin 7—) is isomeric with half-life  $145 \pm 15$  microseconds.<sup>5</sup> Capture takes place almost entirely into two 5— levels at 3280.1 and 3403.5 keV.

Shortly after the publication of the earlier experimental work<sup>3,4</sup> a theory of the energy levels of  $\text{Pb}^{206}$  was proposed by Pryce,<sup>1</sup> based on the shell model and the supposedly known level scheme of the simpler nucleus  $\text{Pb}^{207}$ , and correlated with the experimental data. At that time it was not possible to establish an unambiguous level scheme and little progress was made in the correlation between theory and experiment. To unravel as complex a spectrum as that of  $\text{Bi}^{206}$  it is necessary to measure gamma-ray energies to very high precision, and detailed coincidence measurements are very desirable. The present work has been performed with this intention. As will be seen in Sec. X, the agreement between the predictions of the shell model and the observed level scheme is very good. In addition to the levels actually observed, the theory predicts many more, but their nonappearance can plausibly be explained in terms of low branching probabilities in the de-excitation process following electron capture.

### II. $\text{Bi}^{206}$ CONVERSION ELECTRON SPECTRUM ABOVE 90 KEV

Measurements on the internal conversion electrons above 90 keV occurring in the decay of  $\text{Bi}^{206}$  were made in the 50-cm radius double-focusing spectrometer<sup>6</sup> at the Nobel Institute. This instrument proved to be excellent for these investigations because of its high resolution and luminosity, low background of scattered electrons, and the ease with which precision determina-

\* Research at the Nobel Institute of Physics was supported by a National Science Foundation Fellowship.

† Under contract with the U. S. Atomic Energy Commission.

<sup>1</sup> M. H. L. Pryce, Proc. Phys. Soc. (London) **A65**, 773 (1952).

<sup>2</sup> D. E. Alburger and G. Friedlander, Phys. Rev. **82**, 977 (1951).

<sup>3</sup> D. E. Alburger and G. Friedlander, Phys. Rev. **81**, 523 (1951).

<sup>4</sup> J. A. Harvey, Phys. Rev. **81**, 353 (1951); Can. J. Phys. **31**, 278 (1953).

<sup>5</sup> D. E. Alburger and M. H. L. Pryce, Phys. Rev. **92**, 514 (1953).

<sup>6</sup> Hedgran, Siegbahn, and Svartholm, Proc. Phys. Soc. (London) **A63**, 960 (1950).

tions could be made. Many different runs were carried out under various conditions of source size and strength and spectrometer resolution. Sources were made in the Institute's large cyclotron by bombarding lead targets with an internal beam of deuterons. Carrier-free separations of the bismuth were then performed according to the chemical methods already described<sup>3</sup> and the activity was electroplated on copper foils using a strip of Pt as an anode. The copper foil forming the cathode was soldered to an enamel-coated wire and immersed into the solution. In order to define the area of the active deposit, all other parts of the foil and the solder connection to the lead-in wire were painted with zapon having nail polish added as a visual aid. A potential of 3 volts and plating times between 1 minute and 2 hours were used. Generally there was never any observable spreading of even the lowest energy lines as a result of source thickness.

The first survey run was made at a spectrometer resolution of 0.5 percent using a 6 mm×14 mm sample which had been prepared from activity produced by a 200 microampere-hour bombardment at 25 Mev. Many of the general features of the electron spectrum which had been observed earlier<sup>3</sup> were confirmed but quite a few new lines appeared. Subsequent study showed that many of these new lines decayed at a slower rate than 6-day  $Bi^{206}$ . Reduction of the beam energy to 16 Mev by moving in the cyclotron target to a smaller radius eliminated all of the more slowly decaying lines in later work. Further discussion of these lines will be given in the next section. Two new 6-day transitions found in this run were observed because of the improved resolution, together with two weak  $K$  lines corresponding to gamma rays of 386 and 1596 keV which had been missed in the earlier investigations. In view of the absence of gamma rays able to produce photo-neutrons<sup>7</sup> from deuterium when the detector was exposed to  $Bi^{206}$  sources, the search for new conversion lines was not continued above 2.2 Mev in the double-focusing spectrometer.

Certain portions of the spectrum were then examined in more detail using a 2 mm×14 mm source and a spectrometer resolution of 0.22 percent. One region of particular interest is shown in Fig. 1. It had already been established<sup>3</sup> that the 803.3-keV transition corresponds to the first excited state of  $Pb^{206}$  and that this gamma ray is the same as the one appearing in  $Po^{210}$  alpha decay to  $Pb^{206}$ . A  $K$  to  $(L+M)$  ratio of 3.7 had been obtained for the  $Po^{210}$  internal conversion electrons but a determination of the corresponding ratio for  $Bi^{206}$  was not possible at 1.2 percent resolution owing to the presence of the two  $K$  lines masking the 803-keV  $L$  and  $M$  electrons. Alpha-gamma angular correlation experiments<sup>8</sup> on  $Po^{210}$  by DeBenedetti and Minton suggested that the 803-keV state is  $2+$ , in agreement with the

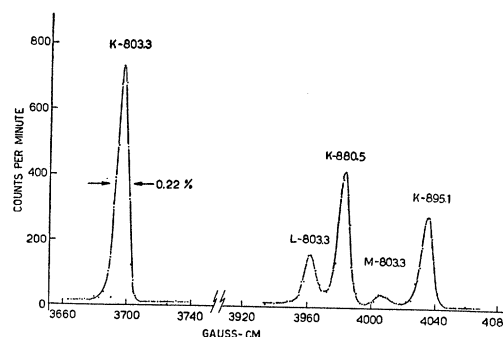


Fig. 1. Conversion electrons of the 803.3-keV transition measured in the double-focusing spectrometer showing the separation of the  $L$  and  $M$  lines from two other  $K$  lines at 0.22 percent resolution.

predicted character of the first excited state of an even-even nucleus.<sup>9</sup> However the  $K$  to  $(L+M)$  ratio of  $Po^{210}$  conversion electrons seemed to be too low for an  $E2$  transition. It was suggested<sup>10</sup> by Goldhaber and Hill that a weak gamma ray of about 880 keV might be present in  $Po^{210}$  decay and if so its  $K$  conversion line could make a contribution to the  $(L+M)$ -803 line thereby accounting for the low  $K$  to  $(L+M)$  ratio observed for the 803 keV transition. In this case the  $(L+M)$  line of the proposed 880-keV gamma would be resolved and might be visible. To test this hypothesis a new 500-Mc  $Po^{210}$  source was obtained through the U. S. Atomic Energy Commission by one of us (D.E.A.) and the conversion electron spectrum of  $Po^{210}$  was re-examined in April, 1952, with the Brookhaven lens spectrometer. A careful search failed to reveal the  $(L+M)$  line of the suggested 880-keV transition. The upper limit placed on a possible 880-keV  $K$ -line intensity, assuming even the largest possible  $K/(L+M)$  ratio, was far too small to affect appreciably the  $K/(L+M)$  ratio of the 803-keV transition. This re-measurement was made at 2 percent resolution and yielded a transition energy of  $804 \pm 3$  keV and a  $K$  to  $(L+M)$  ratio of  $3.8 \pm 0.3$  in agreement with the earlier results. It was concluded<sup>11</sup> that the empirical curves of  $K/(L+M)$  as a function of  $Z^2/E$  may not be accurately valid at high  $Z$ .

Returning to the  $Bi^{206}$  data of Fig. 1 it may be seen that complete resolution of the  $L$  and  $M$  electrons of the 803.3 keV transition is achieved at 0.22 percent resolution. A  $K$  to  $L$  ratio of  $4.8 \pm 0.3$  and a  $K$  to  $(L+M)$  ratio of  $4.0 \pm 0.3$  are obtained from this curve. The latter agrees with the  $Po^{210}$  results discussed above and further confirms that the same transition is involved in both the  $Po^{210}$  and  $Bi^{206}$  decay processes. It is shown in Sec. XI. that this  $K/L$  ratio agrees well with the theoretical value for  $E2$  radiation.

Another part of the spectrum studied at 0.22 percent

<sup>7</sup> E. der Mateosian and M. Goldhaber, Phys. Rev. **78**, 326 (1950).

<sup>8</sup> S. DeBenedetti and G. H. Minton, Phys. Rev. **85**, 944 (1952).

<sup>9</sup> M. Goldhaber and A. W. Sunyar, Phys. Rev. **83**, 906 (1951).

<sup>10</sup> M. Goldhaber and R. D. Hill, Revs. Modern Phys. **24**, 179 (1952).

<sup>11</sup> D. E. Alburger, Phys. Rev. **92**, 1257 (1953).

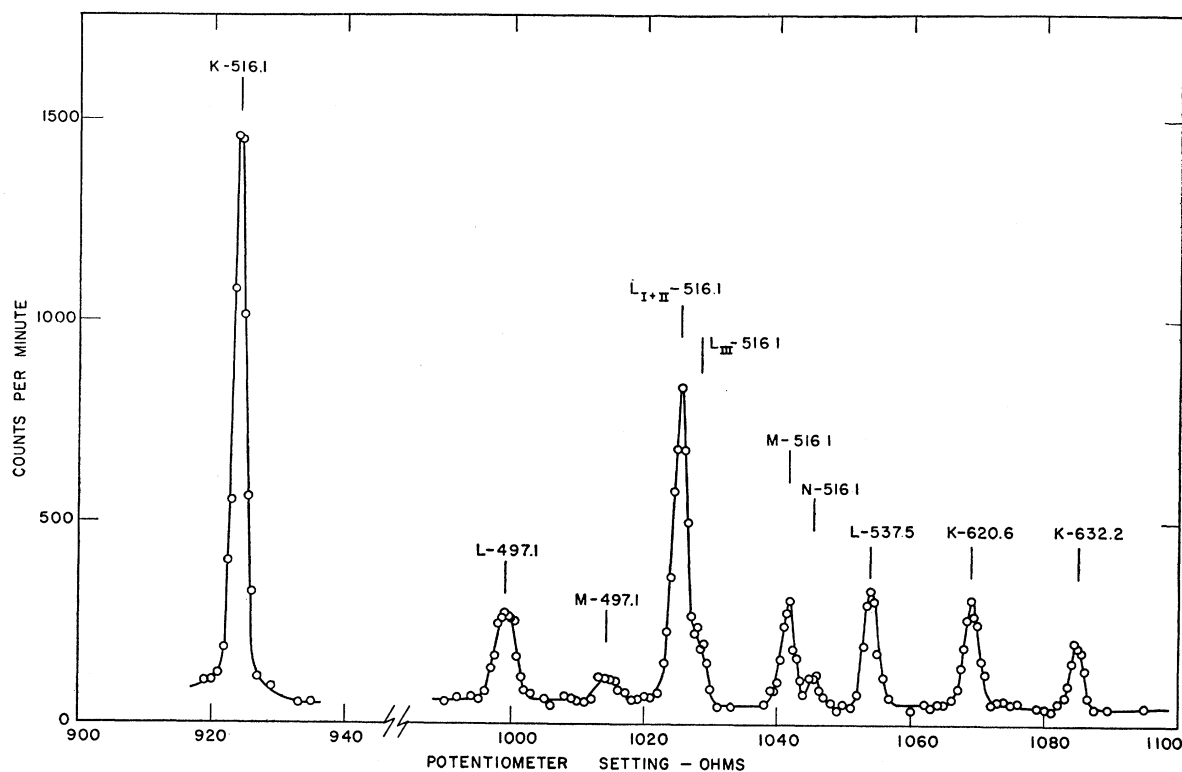


FIG. 2.  $\text{Bi}^{206}$  conversion spectrum at 0.22 percent resolution in the region of lines corresponding to the 516.1-kev 145-microsecond  $E3$  transition.

resolution is given in Fig. 2. This shows a number of lines including the conversion electrons corresponding to the 516.1-kev  $E3$  isomeric transition in  $\text{Pb}^{206}$ . Relative conversion intensities of this transition, given in a report already published,<sup>5</sup> were taken from this figure and are listed again in Table XII together with the theoretical  $K/L_{I+II}$  ratio.

Precision determinations were made on the 19 strongest  $K$ -conversion lines of  $\text{Bi}^{206}$  following techniques similar to those previously developed at the Nobel Institute. The procedure consisted of comparing the extrapolated high-energy momentum edges of the  $\text{Bi}^{206}$   $K$  lines with those of standard sources in the double-focusing spectrometer. Three comparison standards were available whose momenta are known with an accuracy of better than 2 parts in  $10^4$  and which are well spaced with respect to the  $\text{Bi}^{206}$  spectrum. These were the ThF line at  $1388.55 \pm 0.2$  gauss-cm,<sup>12</sup> the  $\text{Cs}^{137}$   $K$ -conversion line at  $3381.28 \pm 0.5$  gauss-cm,<sup>13</sup> and the  $K$ -conversion line of the  $1.3325 \pm 0.0003$ -Mev gamma ray<sup>14</sup> of  $\text{Co}^{60}$  which lies at 5879.2 gauss-cm. After carefully demagnetizing the spectrometer magnet, the high-energy edges of all the  $\text{Bi}^{206}$  lines and the three standards were run in order of increasing

momentum. This required changing sources at the proper point for inserting each standard. To ensure a fixed geometry each source was placed behind a 2-mm wide window whose position in the spectrometer could be reproduced accurately. ThF sources were made by electrostatic collection on copper strips from thorium-active deposit and the  $\text{Co}^{60}$  source was the same as that used in the precision determinations already reported.<sup>14</sup> Two complete sets of comparison runs were made at a resolution of 0.25 percent. Final values were taken from the second run in which the calibration constants of the spectrometer derived from the three standard lines were as follows:

ThF	2.80755 gauss-cm/ohm
$\text{Cs}^{137}$	2.80727 gauss-cm/ohm
$\text{Co}^{60}$	2.80790 gauss-cm/ohm

These figures indicate a surprisingly good linearity of the instrument over a factor of 4 variation of field setting. Because the spread of only 2 parts in  $10^4$  is well within the errors of the absolute values a fixed calibration constant of 2.80757 gauss-cm/ohm was adopted.

It is estimated that the errors of the 19 accurately determined  $\text{Bi}^{206}$  gamma rays given in Group A of Table I are about 5 parts in  $10^4$ . These values were obtained by adding 88.0 kev to the energy of each  $K$  line. In the previous work<sup>8</sup> the conversion electrons had been measured in a lens spectrometer and the

<sup>12</sup> G. Lindström, Phys. Rev. **83**, 465 (1951).

<sup>13</sup> Lindström, Siegbahn, and Wapstra, Proc. Phys. Soc. (London) **B66**, 54 (1953).

<sup>14</sup> Lindström, Hedgran, and Alburger, Phys. Rev. **89**, 1303 (1953).

following transition energies in keV were reported: 182, 234, 260, 341, 396, 470, 505, 536, 590, 803, 880, 889, 1020, 1097, and 1720. Re-examination of the old data revealed that numerical errors had been made in obtaining the energies of the 470 and 505 keV gamma rays, which accounts for the large discrepancies with the values 497.1 and 516.1 keV in Table I. Otherwise the agreement is 1 percent or better for corresponding lines. The 590-keV gamma finds no counterpart in Table I because the strong conversion line from which it had been derived turned out, from the present experiments, to be the  $L$  line of a 516.1-keV isomeric transition rather than  $K$  590. Of the remaining transitions in Group A of Table I, gammas 5 and 18 had been missed in the old work because of their low conversion intensities and 10 and 11 were in an unresolved region. The  $K$  line of number 12 had been observed but no interpretation was given.

In further work with the double-focusing spectrometer, a strong source was prepared from a sample made at 16-MeV bombarding energy. A number of new and very weak 6-day lines was observed, some of which were only 10 percent as strong as the background rate. Their transition energies which are given in Group B of Table I were determined, except for the 123.6-keV transition, from the positions of the  $K$  peaks referred to the neighboring and more accurately measured  $Bi^{206}$  lines listed in Group A of Table I. A resolution of about 0.5 percent was used and errors were estimated to be of the order of 0.15 percent. The 123.6-keV transition was determined by interpreting the observed electron line as  $L$ -123.6. Later the corresponding  $K$  line was found with the intermediate-image spectrometer. Among the gamma rays given in Group B of Table I, the  $K$  line of the 816.3-keV transition was barely visible making this the only doubtful gamma ray on the list. Relative conversion intensities and  $K/L$  ratios are discussed in Sec. XI. There was only one weak electron line observed in the double-focusing spectrometer, having an energy of 102.2 keV, to which no firm assignment has been made.

TABLE I.  $Bi^{206}$  transition energies in keV.

A. From $K$ -line determinations accurate to 5 parts in $10^4$ .			
1.	184.1	8.	516.1
2.	234.3	9.	537.5
3.	262.8	10.	620.6
4.	343.4	11.	632.2
5.	386.0	12.	657.3
6.	398.1	13.	803.3
7.	497.1	14.	880.5
B. From $K$ -line determinations accurate to 1.5 parts in $10^3$ .			
20.	123.6	24.	753.9
21.	202.5	25.	816.3
22.	313.6	26.	841.7
23.	739.9		

### III. CONVERSION ELECTRON SPECTRUM OF 14-DAY $Bi^{206}$

As mentioned in the preceding section, the first survey run on the bismuth spectrum revealed a number of lines which decayed at a slower rate than 6-day  $Bi^{206}$ . Since the source had been made at 25 MeV it was suspected that these lines might be associated with  $Bi^{205}$  formed by the  $Pb^{206}(d,3n)Bi^{205}$  reaction. A study over a period of several weeks showed that all but one pair of lines, (the  $K$  and  $L+M$  lines associated with the 1064-keV transition<sup>11</sup> in the decay of 50-year  $Bi^{207}$ ) were decaying with a half-life approximately twice as long as that of  $Bi^{206}$  or consistent with the 14.5-day period<sup>15</sup> of  $Bi^{205}$ . It was reasoned that if the  $(d,3n)$  reaction were responsible, the threshold would be high and production of this isotope would not occur at a lower bombarding energy. Later a bismuth source from a 16-MeV bombardment was examined and only very slight indications of even the strongest of these 14-day lines were detected. It was concluded that if the isotope and reaction assignments were correct, then the  $Pb^{206}(d,3n)$  threshold must be in the neighborhood of 16 MeV.

Table II gives the energies, relative  $K$ -line intensities, and approximate  $K/L$  ratios of these transitions. The energies, which are accurate to about 0.2 percent, seem to have little, if any, correlation with the  $Bi^{206}$  gamma rays of 0.431, 0.527, 0.550, 0.746, and 1.84 MeV reported<sup>16</sup> by Karraker and Templeton. Of their values the last is close to  $h$  of Table II but it would then be difficult to understand why the much stronger 1766.3-keV transition had not been observed. More recently Wapstra has reported<sup>17</sup> a 1.77-MeV gamma ray in bismuth sources made by 27-MeV deuteron bombardment of lead and tentatively assigns this to  $Bi^{205}$  from its decay rate. His gamma ray probably corresponds to  $i$  of Table II.

The  $K/L$  ratios given in Table II cannot be considered as very satisfactory inasmuch as only one run

TABLE II. Data on 14-day lines assigned to  $Bi^{205}$ .

	$E_\gamma$ (keV)	Relative $K$ -line intensity	$K/L$
a.	284.4	100	
b.	703.7	87	$\sim 5$
c.	911.6	8.9	
d.	988.6	22	
e.	1044.6	31	$\sim 4$
f.	1074.1	2.9	
g.	1189.8	4.0	$\sim 4$
h.	1615.4	2.4	$\sim 4$
i.	1766.3	40	5.8
j.	1777.8	4.4	
k.	1864.2	1.6	$\sim 5$

<sup>15</sup> Hollander, Perlman, and Seaborg, Revs. Modern Phys. 25, 469 (1953).

<sup>16</sup> D. G. Karraker and D. H. Templeton, Phys. Rev. 81, 510 (1951).

<sup>17</sup> A. H. Wapstra, thesis, Amsterdam, 1953 (unpublished).

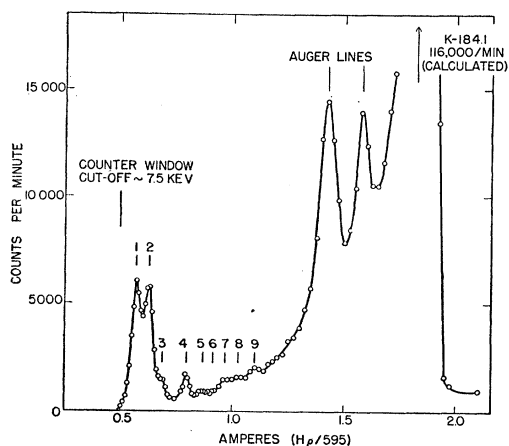


FIG. 3. The low-energy electron spectrum of  $\text{Bi}^{206}$  as observed in the intermediate-image spectrometer.

was made and furthermore the presence of many  $\text{Bi}^{206}$  lines made the measurements inaccurate. A possible isomeric transition in  $\text{Pb}^{205}$  is not suggested by the conversion data.

Although it is too early to propose a decay scheme for  $\text{Bi}^{205}$ , there are three cascade crossover relationships, given in Table III, which hold within the errors of measurement. From these several possibilities for the level scheme of  $\text{Pb}^{205}$  suggest themselves, one of which would include states at 703.7, 988.6, 1615.4, and 1777.8 keV. There may well be other 14-day lines which were too weak to be observed in the present investigation. A suggested way of studying the spectrum would be to make an intense bombardment of lead with deuterons  $\sim 25$  MeV and then allow the target to decay before performing the chemical separation and spectrometer runs. Each month of decay would reduce the amount of  $\text{Bi}^{205}$  by a factor of 4 but at the same time the  $\text{Bi}^{205}/\text{Bi}^{206}$  ratio would increase by a factor of 4. After a suitable period the spectrum would be relatively free of  $\text{Bi}^{206}$  and there might be hope of making a more conclusive examination of the  $\text{Bi}^{205}$  conversion electrons and perhaps even doing coincidence experiments.

#### IV. LOW-ENERGY LINES OF $\text{Bi}^{206}$ —AUGER INTENSITIES

In order to have more complete information on the entire conversion spectrum of  $\text{Bi}^{206}$ , the investigation of electron energies was extended below 96 keV by means of the Slätis-Siegbahn intermediate-image spectrometer<sup>18</sup> at the Nobel Institute. This instrument is more satisfactory than the double-focusing spectrometer at very low energies if only moderate resolution is desired. The spectrum was run according to standard procedures using a 0.5-cm diameter electroplated source, a spectrometer resolution of 4 percent, and a counter window with a 7.5-keV cutoff. Figure 3 shows the results

obtained. Unfortunately the peaks labelled 5, 6, and 8 do not show up well in the drawing but these could be reproduced consistently in three separate studies which were made to establish that all of the lines were decaying with a half-life of 6 days. The energies of the lines and their intensities are listed in Table IV. It is estimated that the momentum values from which the energies were derived are accurate to 2–3 percent. This is consistent with the observed energies of the main Auger groups which, according to known binding energies, should be

$$(K-L) - L \cong 57 \text{ keV},$$

$$(K-L) - M \cong 69 \text{ keV}.$$

Intensities are given in electrons per 100 disintegrations, this normalization having been made by measuring the  $K$ -803.3 line and assigning the latter a value of 0.85 electron per 100 disintegrations as in Table XI. Since the peak heights were taken rather than areas the actual total  $K$  Auger intensity is probably greater than the 3 percent indicated by Table IV.

It is of interest to consider the  $K$  Auger intensity in relation to the decay scheme.  $K$  x-rays or Auger electrons can arise following either  $K$  electron capture or internal conversion in the  $K$  shell. According to the sum of numbers in column 4, Table XI, internal conversion produces  $K$ -shell vacancies in about 45 percent of the disintegrations. Massey and Burhop have calculated<sup>19</sup> the internal conversion probability of  $K_\alpha$  x-rays and find this to be 5 percent at  $Z=82$ . Taking the gamma-ray data into account, the  $K$  Auger yield would be 7 percent if all of the primary excitations involved  $K$  electron capture, or 2 percent if only  $L$  capture occurs. Because of the large probable errors in the intensities of these low energy lines and the likelihood that the  $K$  Auger intensities given in Table IV are low, the experimental results cannot be used as an argument that there is only a small amount of  $K$  capture. Without more accurate data it is not possible to derive a meaningful value for the ratio of  $K$  to  $L$  capture or information about the disintegration energy which might be derived from such a ratio.

The only two low-energy lines to which definite assignments have been made, except for the Auger lines, are Nos. 4 and 9. No. 9 seems to fit as the  $K$  line of the 123.6-keV gamma ray whose  $L$  line was observed

TABLE III.  $\text{Bi}^{205}$  Cascade cross-over relations derived from the transitions listed in Table II.

Gamma	Sum (keV)	Possible crossover	Difference in energy (keV)
$a+b$	988.1	$d$	0.5
$b+c$	1615.3	$h$	0.1
$b+f$	1777.8	$j$	0.0

<sup>18</sup> H. Slätis and K. Siegbahn, *Arkiv Fysik* **1**, 339 (1949).

<sup>19</sup> H. W. S. Massey and E. H. S. Burhop, *Proc. Roy. Soc. (London)* **A153**, 661 (1936).

as mentioned in Sec. II while No. 4 is the proposed  $K$  line of a 107.2-keV gamma. It is possible that No. 8 is the  $K$  line of a 117-keV gamma whose  $L$  line is the previously unassigned 102.2-keV electron found in the double-focusing spectrometer. On the other hand the 102.2-keV line may be an  $M$  line corresponding to the 107.2-keV transition proposed above. Energetically, lines 1, 2, and 3 could be Auger electrons arising from  $L$ -shell vacancies. There does not seem to be enough published information on  $L$  Auger effects to establish such assignments, particularly in regard to the intensities of such lines relative to the  $K$  Auger peaks. Judging from the appearance of Fig. 3 it is likely that other unresolved lines exist in  $Bi^{206}$  at these low energies and, if so, a study at higher resolution would be profitable.

#### V. SEARCH FOR POSITRONS FROM $Bi^{206}$

During the course of the low-energy conversion line measurements with the intermediate-image spectrometer described in the preceding section, an attempt was made to detect positrons emitted in the decay of  $Bi^{206}$ . A set of spiral baffles already present in the instrument served to reject positive or negative electrons as desired. Using the same source and apertures as in the preceding section, counts were taken at a number of current settings between 300 and 7500 gauss-cm (8 keV to 1.8 MeV). An upper limit of 10 counts per min could be placed on the yield of positrons at any point over this region. Considering the 4-percent spectrometer resolution any positron distribution whose maximum lay below 1.8 MeV could have been detected if the integrated spectrum contained more than 200 positrons per min. The yield of the  $K$ -803.3 line with the current reversed was 4460 counts per min. Since this transition occurs once per disintegration and is 0.85 percent converted in the  $K$  shell (see Sec. XI) one can conclude that the maximum number of positrons per disintegration is  $200/(4450 \times 117) = 1/2600$ .

#### VI. SPECTROGONIOMETER COINCIDENCE EXPERIMENTS

With so many transitions occurring in  $Bi^{206}$  decay it became apparent that coincidence studies would be of great assistance in formulating a decay scheme. At first sight it appeared from the complexity of the conversion spectrum that reasonably good resolution would be required in both sections of the apparatus and that coincidences between  $K$  conversion electrons would be the most profitable thing to look for.

Available for this purpose was a two-lens spectrometer, or "spectrogoniometer," designed by Professor Kai Siegbahn<sup>20</sup> and located at the Royal Institute of Technology in Stockholm. This instrument can be used for studies of coincidences between electrons of separately selected energy and in addition the angular correlation of these electrons can be measured between

TABLE IV. Low-energy electron lines of  $Bi^{206}$ . Numbers refer to peaks in Fig. 3.

Line	Energy (keV)	Intensity (electrons per 100 disintegrations)*
1	10.2	0.99
2	12.3	0.89
3	14.3	0.23
4	19.2	0.23
5	23.2	0.05
6	26.0	0.02
7	28.8	0.08
8	31.8	0.04
9	36.2	0.07
Auger 1	58.6	1.8
Auger 2	71.1	1.1

\* Taken from peak height. No window corrections have been made.

90° and 180°. The latter feature was not used in the present experiments which were always performed at 180°. Prior to this work the instrument had been modified by Professor Siegbahn to use anthracene crystal detectors in conjunction with magnetically shielded RCA 5819 photomultipliers, and to use a coincidence circuit of  $\sim 8 \times 10^{-8}$  sec resolving time. The crystals were located inside the vacuum chamber and were optically connected to the 5819's by Lucite end windows approximately 5 mm thick. At the lowest electron energy studied (96 keV) the pulses obtained were large enough to operate the coincidence circuit satisfactorily. Otherwise the performance features of the instrument such as the 0.3 percent transmission at 3 percent resolution of each section, were the same as those already given.<sup>20</sup> The effect of resolution is shown in Fig. 4 which compares the three neighboring  $K$  conversion lines of 497.1-, 516.1-, and 537.5-keV transitions as seen in the double-focusing spectrometer at 0.5 percent resolution, the spectrogoniometer at 3 percent, and the intermediate-image spectrometer at 5.5 percent resolution.

Mounting of the sources had to be considered carefully since one of the spectrometers detects electrons which have passed through the source backing. In order to retain the electroplating method a thin copper foil was to be preferred. Suitable foils were prepared by rolling copper sheet down to 7 mg/cm<sup>2</sup> and then dipping these in a weak solution of nitric acid until the thickness was reduced to 2.5–3 mg/cm<sup>2</sup>. The presence of many pinholes was evidence of considerable non-uniformity of the foils. For mechanical support each foil was soldered to a 2.2-cm diameter brass ring fitting the spectrometer source holder. Electroplating of the activity was then carried out in the usual manner after painting the backing with a zapon nail-polish mixture except for a 0.5-cm diameter central area where the bismuth was deposited. When the plating was completed the zapon on the foil immediately behind the source spot was dissolved off in order to remove unnecessary material.

The effect of the backing on the electrons passing

<sup>20</sup> K. Siegbahn, Arkiv Fysik 4, 233 (1952).

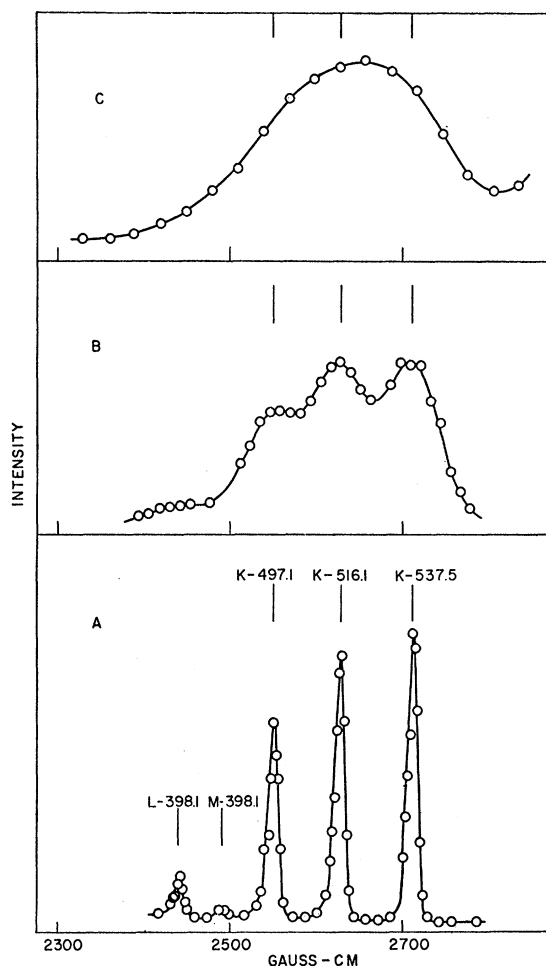


FIG. 4.  $\text{Bi}^{206}$   $K$ -conversion electrons of the 497.1-, 516.1-, and 537.5-keV transitions as observed in the double-focusing spectrometer at 0.5 percent resolution, curve *A*; one section of the spectrogoniometer at 3 percent resolution, curve *B*; and the intermediate-image spectrometer at 5.5 percent resolution, curve *C*.

through it is shown in Fig. 5 for two  $K$  lines of 96-keV and 255-keV energy. Comparison with the curves taken when the activity side was facing the spectrometer shows that the backing causes a considerable distortion of the 96-keV peak but has relatively little effect on the 255-keV peak. In the latter case the line is shifted by about 3 keV consistent with the 2.5-mg/cm<sup>2</sup> average thickness of the copper. Coincidence studies involving the 184.1-keV transition were always made with its  $K$  line entering that spectrometer on the source side of the foil.

With each spectrometer set on the peak of a  $K$  line the coincidence rate was measured and compared with the random rate calculated from the singles and the known coincidence resolving time. In the region shown in Fig. 4 the momentum resolution was sufficient to establish separately the coincidence effects at each peak. However, many of the other  $K$  lines were not resolved well enough or were too weak to be accessible

to this type of measurement. In the latter case the random rate proved to be a limitation. For example, although a net coincidence rate equal to the random rate between  $K$ -537.5 and  $K$ -803.3 could be observed, no definitive results could be obtained when  $K$ -803.3 and  $K$ -880.5 (with  $K$ -895.1 unresolved) were focused. It was concluded from later knowledge of the multipole orders of these gammas that the coincidence effect between two transitions whose conversion coefficients are both  $\leq 1$  percent is difficult to establish in this instrument. From the point of view of coincidence experiments the 6.4-day half-life of  $\text{Bi}^{206}$  is rather ideal, since it is long enough to allow good data to be taken and analyzed yet short enough to permit any given pair of lines to be studied under optimum conditions within a reasonable time.

The results of these experiments are given in Table V. It was not possible to reproduce the coincidence rate of a given pair to better than 50-percent accuracy in widely separated runs. The relative intensity figures given in Table V may therefore be in error as much as a factor of 2. Also listed in the table are the noncoincident pairs, those for which a yield might have been expected on the basis of the line intensities, but which showed no effect above the background rate. Evidently these cases impose equally important restrictions on the decay scheme.

It may be seen from a consideration of Fig. 1 that the  $K$ -880.5,  $K$ -895.1,  $L$ -803.3, and  $M$ -803.3 lines are unresolved in the spectrogoniometer because of the 3 percent resolution. While the 343.4-880.5 and 343.4-895.1 pairs have been listed under the "no coincidences" column of Table V, actually coincidences were observed in these runs. The ratio of the  $K$ -343.4- $K$ -803.3 coincidences to the rate measured between  $K$ -343.4 and this unresolved group was  $3.5 \pm 1.5$ . Since this figure is consistent with the  $K/(L+M)$  ratio of the 803.3-keV transition derived from Fig. 1, all coincidences with the unresolved group in this case could be attributed to the 803-keV  $L$  and  $M$  electrons. A similar situation arose when the  $K$ -537.5 line was studied together with the  $K$ -803.3 line and the unresolved group mentioned above, but in this case the ratio was about 2 and the

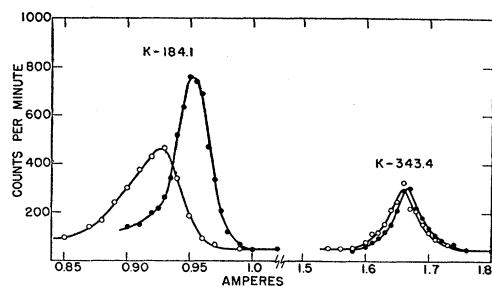


FIG. 5. Electron lines of 96 and 255 keV observed in the spectrogoniometer to study the effect of source backing. Solid points—direct observation. Open circles—electrons observed after passing through the backing.

statistical errors were relatively large. If the  $L$  and  $M$  electrons of the 803.3-keV transition had not been resolvable otherwise, measurements such as those described here would have been a way to obtain the  $K/(L+M)$  ratio in spite of complete masking of the  $L$  and  $M$  lines.

### VII. ELECTRON-GAMMA COINCIDENCE MEASUREMENTS

When it was first suspected that one or both of the highest energy transitions in the decay of  $Bi^{206}$  might be in coincidence with other gamma rays in the decay scheme, it was realized that a limited number of coincidence experiments could be done which would not require good resolution in both parts of the apparatus, such as the work described in preceding section. An examination of the strong transitions listed in Group *A* of Table I shows that gammas No. 18 and No. 19 are 50 percent higher in energy than their nearest neighbor. This suggested looking for coincidences between  $K$ -conversion lines and the output of a NaI gamma-ray detector biased so as to respond only to the more energetic radiation.

The equipment selected for this work was the Slätis-Siegbahn intermediate-image beta-ray spectrometer<sup>18</sup> which can be operated at 4 percent resolution when the transmission is 8 percent. Other experiments on  $Bi^{206}$  using this instrument have already been described in Secs. IV and V. A spare source-end pole piece of the spectrometer incorporating a NaI crystal and EMI photomultiplier detector was available and had been tested by Dr. J. Moreau. The photomultiplier was equipped with an iron shield and inserted into a large hole machined through the pole piece such that the NaI crystal, held in contact with the face of the tube, came to within several cm of the normal source position. Its location did not result in a very favorable solid angle subtended at the source (i.e., <10 percent) but further insertion would have had a serious effect on the gain of the photomultiplier. A light-piping arrangement had not been constructed at that time. In the photomultiplier position chosen, the variation

TABLE V.  $Bi^{206}$  coincident and noncoincident transitions from electron-electron measurements. Gamma energies in keV.

Coincident pair	Coin./min	No coincidences observed
184.1—262.8	4.0	184.1—343.4
184.1—398.1	10.0	184.1—516.1
184.1—497.1	2.5	184.1—537.5
184.1—880.5	0.74	184.1—803.3
and/or 895.1		
184.1—1018.8	0.5	343.4—398.1
343.4—497.1	1.2	343.4—880.5
343.4—516.1	3.4	343.4—895.1
343.4—537.5	7.0	398.1—516.1
343.4—803.3	0.66	398.1—537.5
398.1—497.1	1.2	537.5—880.5
537.5—803.3	0.23	537.5—895.1

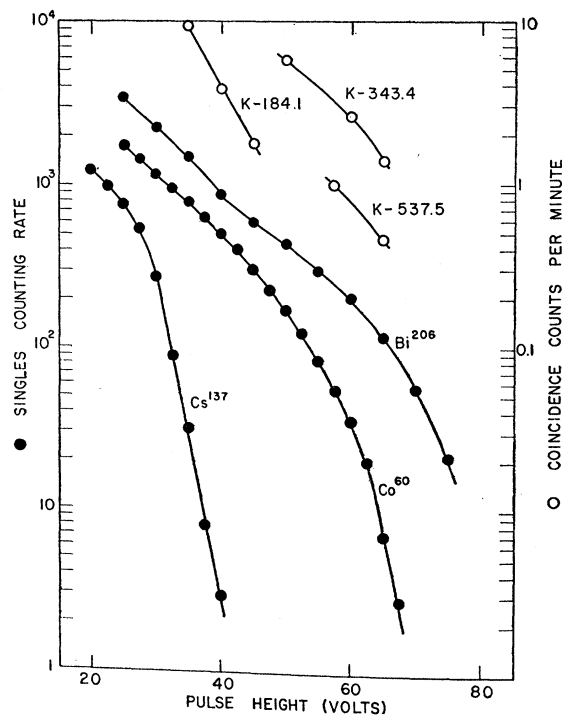


FIG. 6. Integral discriminator curves obtained with the NaI detector used in the electron-gamma coincidence measurements. Curves with solid points are for  $Cs^{137}$ ,  $Co^{60}$ , and  $Bi^{206}$ . Open circles indicate the change of coincidence rate with discriminator setting when three different  $K$  lines were focused.

of the magnetic field from zero to full current caused a pulse-height shift of about 10 percent when  $Co^{60}$  gamma rays were measured.

A decrease in the resolution of the intermediate-image spectrometer from 4 percent to 5.5 percent when using the largest aperture and a 5-mm diameter source was observed in going from the normal source-end pole piece to the modified one described above. Apparently this was the result of a less favorable magnetic field distribution caused by the large hole for the photomultiplier. Curve *C* of Fig. 4 shows how the 5.5 percent resolution affected one important region of the conversion spectrum.

The outputs of the spectrometer Geiger counter and the crystal detector discriminator were fed to a coincidence circuit having a resolving time of 0.4 microsecond.  $Bi^{206}$  sources which had been used in the spectrogoniometer measurements were of the proper size and had decayed to the point where they could be employed for these experiments.

Figure 6 shows the NaI detector integral pulse-height distributions taken with  $Cs^{137}$ ,  $Co^{60}$ , and  $Bi^{206}$  sources. These have not been normalized as regards intensity since the main feature of importance here is the rate of falloff in a given pulse-height range. The  $Bi^{206}$  curve clearly shows the presence of gamma rays more energetic than the 1.3-MeV  $Co^{60}$  radiation and also gives some evidence of complexity.



In the first tests, coincidences between  $K$ -conversion lines focused in the spectrometer and the NaI crystal detector output were looked for when the discriminator was set to accept pulses of amplitude greater than 55 volts. (See Fig. 6.) Four  $K$  lines gave effects well above the calculated random rates while five did not. These are listed in Table VI together with the net counting rates.

It was important to establish that the effects observed were caused by the high-energy part of the  $\text{Bi}^{206}$  gamma-ray spectrum and not by pile up of small pulses or by the discriminator curve tail of lower-energy gamma rays. The possibility of pile up was excluded by measuring the coincidences over a period of a week. The rates were found to decrease with the  $\text{Bi}^{206}$  half-life. Effects of the discriminator curve tail of lower-energy gammas were eliminated by studying the variation of the coincidences with the discriminator pulse-height setting. It is seen from the curves labeled  $K$ -343.4 and  $K$ -537.5 in Fig. 6 that these rates follow closely the shape of the high-energy portion of the  $\text{Bi}^{206}$  singles spectrum. On the other hand, coincidences with the  $K$ -184.1 line found in the vicinity of 40 volts, as shown in Fig. 6, fall off in such a way as to correspond to gamma-rays having energies intermediate between those of  $\text{Cs}^{137}$  and  $\text{Co}^{60}$ . According to any reasonable extrapolation of the  $K$ -184.1 curve the coincidence rate at 55 volts would not be detectable above background in agreement with the measurements at this setting. The rates of change of the 803.3 and 880.5 coincidences with discriminator setting were not studied because of the low yield. These lines have been assigned as being in coincidence with the high-energy gammas since the yields of all 4 lines in Table VI at a pulse-height setting of 55 volts are in proportion to the relative  $K$ -line intensities.

One other possibility is the effect of pulse addition in the crystal. Thus two members of a triple cascade might give a large pulse which would account for the observed distribution of yield with discriminator setting indicated in Fig. 6. Because of the small solid angle for gamma detection and the low efficiency imposed by the size of the NaI crystal ( $\sim\frac{1}{2}$  inch cube), it was not thought that pulse addition could have accounted for the yields observed.

TABLE VI. Coincidence effects between the 1596.3 and/or 1719.7-keV gamma rays and the  $K$ -lines of other transitions at a discriminator setting of 55 volts (see Fig. 6). Gamma energy in keV.

Coincidences observed	Counts per min	No detectable coincidences
343.4	3.2	184.1
537.5	0.96	262.8
803.3	0.35	497.1
880.5	0.21	516.1
and/or 895.1		1018.8

It might be questioned how the coincidence or noncoincidence effects listed in Table VI for the 497.1-, 516.1-, and 537.5-keV gamma rays could be established when their individual  $K$  lines were not resolved (see Fig. 4). The net coincidence rates when the spectrometer was set at the momenta corresponding to the three peaks were as follows: 537.5—0.96/min, 516.1—0.61/min, and 497.1—0.10/min. A plot of these rates shows that they are roughly consistent with the shape of a conversion line of 5.5 percent half-width centered at the  $K$ -537.5 position. While coincidences with the two lower-energy lines cannot be excluded entirely it seems improbable that they occur.

Several cases other than those listed in Table VI were examined but no conclusive results were obtained. The experiments were limited by the spectrometer resolution or by low yields. The  $K$ -398.1 line could not be studied because of the unresolved  $L$  and  $M$  electrons of the 343.4-keV transition, already known to be in coincidence from measurements on the  $K$ -343.4 line.

#### VIII. MEASUREMENT OF THE 145-MICROSECOND ISOMERIC LIFETIME

A report has already been given<sup>5</sup> on the discovery of a 145-microsecond isomeric state in  $\text{Pb}^{206}$  decaying by  $E3$  transitions of 516.1 or 202.5 keV. Revised values of the relative conversion intensities are discussed in Sec. XI. The lifetime measurements were made at the Nobel Institute with a triggered oscilloscope (Tektronix-type 511AD synchroscope) connected through an amplifier and discriminator to the output of a NaI crystal and EMI photomultiplier. The detector was exposed to a weak source of  $\text{Bi}^{206}$  and the delayed pulse distribution was measured by counting the number of pulses appearing in a slot of fixed width placed over the face of the scope at various distances from the origin pulse. A 10-cm, 500-microsecond base line was used, while the slot width was 1.5 cm corresponding to an interval of 75 microseconds. Recording of the data was done electrically by focusing the image of the scope screen with a large lens onto a 931 photomultiplier whose circuit was designed to avoid spurious pulses from the decay of the scope screen phosphor. The resulting delayed pulse distribution, after subtraction of a calculated random rate, is given in Fig. 1 of reference 5. This shows the presence of a state having a half-life of  $145 \pm 15$  microseconds.

Several further details of these measurements might be worth mentioning. One difficulty in recording the data was caused by background light on the scope screen. An intensity blanking circuit was not available and at the low triggering rates ( $\sim 25/\text{sec}$ ) there was a tendency for the flickering of the background light to cause spurious counts from the 931 photomultiplier. This trouble was minimized as described in the following. The discriminator output pulses, all of equal size, were fed to the scope amplifier whose gain was set at

maximum. Saturation of the amplifier in this manner resulted in pulses whose light was concentrated mostly at the top giving the appearance of detached spots on the screen above the base line. The height of the 1.5-cm wide movable slot was narrowed down to 5 mm and its vertical position was adjusted to a height above the base line such that only these spots could be seen. In this way the ratio of the intensity of light associated with a pulse to the intensity of background light was increased to the point where reliable operation was achieved.

An important part of the measurements was the calibration of the base line. This was done by presenting on the scope screen a 200-kc/sec sine wave from a G. R.-type 805C signal generator. Without disturbing the optical lens, the 931 photomultiplier pulse-detector tube was removed and the image of the scope screen formed by the lens was observed with the aid of a low-power microscope borrowed from the Institute's large comparator. The number of cycles was then counted for each position of the same 1.5-cm wide cardboard mask as employed in taking the delayed pulse distribution. On the average 15 cycles appeared in the slot and these could be counted with an accuracy of about  $\frac{1}{3}$  of a cycle. The calibration carried out in this way effectively eliminated all parallax errors inasmuch as the microscope saw closely the same sweep interval as the photomultiplier. It was found that the inherent nonlinearity of the scope sweep combined with the effect of curvature of the tube face required corrections of up to 20 percent near the ends of the trace. Unfortunately it could not be determined whether or not the sweep rate when the calibrating sine wave was impressed was slightly different than under the pulse conditions of the experiment. An accurate pulser time base would have been more suitable for calibration purposes. Actually a more satisfactory determination of the half-life could be made with a larger NaI crystal together with a pulse-time channel analyser.

#### IX. CONSTRUCTION OF THE TERM DIAGRAM OF $Pb^{206}$ —ENERGIES

With the exception of the weak unassigned electron line of 102.2 keV mentioned in Sec. II and seven of the very low-energy lines discussed in the Sec. IV, the results described thus far all fit in with the  $Pb^{206}$  level scheme shown in Fig. 7. This has 10 excited states whose energies, spins, and parities can be assigned with fair certainty and two additional states whose energies, spins, and parities are probable.

Construction of the term diagram was started by assuming  $0+$  for the ground state and by assigning an energy of 803.3 keV and a spin and parity of  $2+$  to the first excited state because of the evidence previously discussed in Sec. II. All of the transitions listed in Table I were then considered for possible cascade crossovers involving three or more gamma rays.

TABLE VII. Double cascade crossover relationships involving sums less than 1720 keV. Gamma numbers from Table I.

	Gamma No.	Sum (keV)	Possible crossover gamma No.	Difference (keV)	Agreement with scheme
A. a.	2 +3	497.1	7	0.0	Yes
b.	2 +5	620.3	10	0.3	Yes
c.	2 +6	632.4	11	0.2	Yes
d.	3 +11	895.0	15	0.1	Yes
e.	4 +9	880.9	14	0.4	Yes
f.	5 +11	1018.2	16	0.6	Yes
g.	6 +7	895.2	15	0.1	Yes
h.	6 +10	1018.7	16	0.1	Yes
i.	7 +17	1595.7	18	0.6	Yes
j.	10 +17	1719.2	19	0.5	Yes
B. k.	1 +11	816.3	25	0.0	Yes
l.	1 +12	841.4	26	0.3	No
m.	1 +22	497.7	7	0.6	No
n.	3 +20	386.4	5	0.4	Yes
o.	4 +7	840.5	26	1.2	No
p.	4 +22	657.0	12	0.3	Yes
q.	4 +24	1097.3	17	1.3	No
r.	5 +16	1404.8	27	0.4	No
s.	7 +20	620.7	10	0.1	Yes
t.	9 +21	740.0	23	0.1	No
u.	15 +20	1018.7	16	0.1	Yes
v.	15 +21	1097.6	17	1.0	No
w.	18 +20	1719.9	19	0.2	Yes
x.	21 +22	516.1	8	0.0	Yes
y.	21 +25	1018.8	16	0.0	No
z.	22 +27	1718.8	19	0.9	Yes
aa.	24 +26	1595.6	18	0.7	Yes
C. bb.	107.2+11	739.4	23	0.5	Yes

Pairs of gamma rays whose sums were less than 1720 keV were examined first. These may be divided into two classes—those derived from the 19 accurately measured transitions (Group A of Table I) and others including all 27 gammas of Table I. In the first class there are 126 possible pairs of lines and of these the sum energies of the ten cases listed in Group A of Table VII agree with a third gamma-ray of Group A of Table I within the combined probable errors of the measurements. Every one of these is consistent with the level scheme. Three relations somewhat outside the errors, are the following:

$$1+10=804.7; \Delta E=1.4,$$

$$3+10=883.4; \Delta E=2.9,$$

$$5+7=883.1; \Delta E=2.6.$$

The fact that cascade crossovers corresponding to these can be rejected illustrates the importance of precision measurements in the interpretation of this very complex spectrum.

When all 27 transitions of Table I are considered, there are 266 pairs of gammas having sums less than 1720 keV. Group B of Table VII lists 17 cases which fall within the errors and involve the less accurately measured gamma rays given in Group B of Table I. Nine of these agree with the scheme while 8 do not. If the level diagram is correct, then the latter are chance additions arising from the large number of possibilities and the lower accuracy of the measurements. In

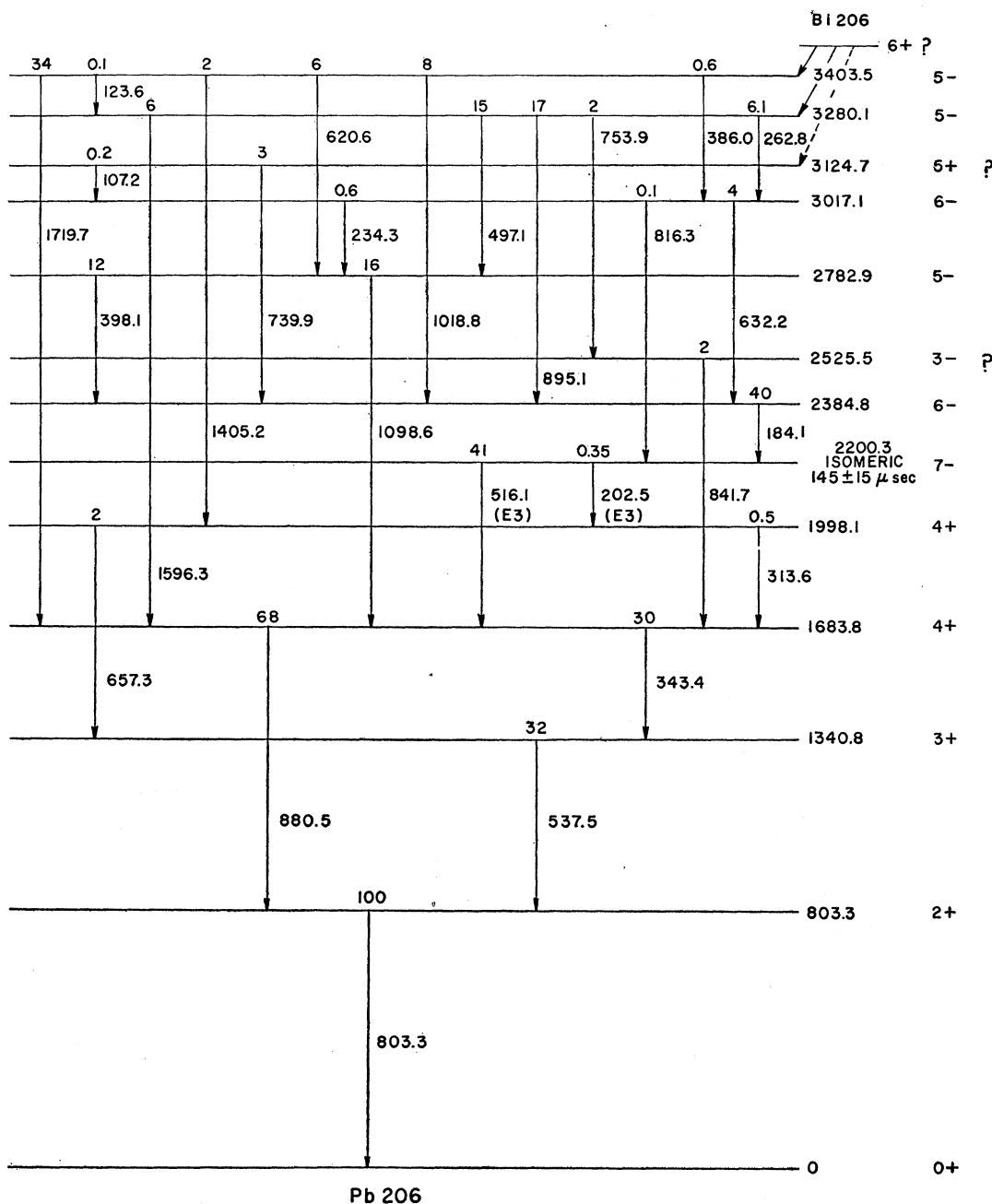


FIG. 7. Energy levels and transitions in  $Pb^{206}$ . The number at the head of each transition is its intensity in percent per disintegration.

addition, if line 4 of Table IV is interpreted as the *K* line of a 107.2-keV gamma ray, there is one further cascade crossover, which is listed as *C* of Table VII.

Triple cascades were also considered but here the analysis becomes more ambiguous because of the very large number of possibilities. For example, the 19 transitions listed in Group *A* of Table I can be combined in more than 300 ways to yield triple sums less than 1720 keV. Some triple sums can be derived directly

from the double sums listed in Table VII. Aside from these there are three relations which agree with the scheme, while four do not agree and must be considered as chance additions. Triple sums involving all 27 transitions of Table I have not been analyzed.

Although the scheme does not necessarily have to follow all of the sum relationships, it must in every case be consistent with well-defined coincidence measurements. The coincidence results described in Secs.

VI and VII together with the isomer measurements discussed in Sec. VIII and the cascade crossover data cited in Table VII were largely responsible for the level arrangement adopted. Inspection shows that all 31 of the coincidence or noncoincidence results listed in Tables V and VI are in accordance with the decay scheme. While it has already been mentioned in Sec. VII that the relative gamma-electron coincidence rates are consistent with the scheme, no detailed analysis of the electron-electron coincidence rates given in Table V has been made.

#### X. CONSTRUCTION OF THE TERM DIAGRAM OF $Pb^{206}$ —SPINS AND PARITIES—CORRELATION WITH THE SHELL MODEL

The energies of the levels in the term diagram can be deduced uniquely from the experimental material alone, except for the two doubtful levels at 2525.5 and 3124.7 keV. All the other levels are involved in at least three transitions, eight in at least four and one (1683.8) in as many as eight transitions. The ground state is involved in only the 803.3-keV transition, and it was fortunate that it was known at the outset that this transition was from the first excited state, although the coincidence measurements also fix its position unambiguously. The spins and parities of the well-established levels could probably also have been deduced from the experimental data alone by using the  $K/L$  ratios, the conversion line intensities, and the calculated conversion coefficients<sup>21</sup> to evolve a consistent scheme of multipole orders and transition intensities, but in practice this would have been difficult. Instead, the predictions of the shell model were used as a guide and were found to be very helpful. Later the intensities were employed to clear up doubtful points.

Those energy levels of  $Pb^{206}$  which do not involve the excitation of nucleons from the closed shells can be treated as arising from a system of two neutron holes. If one knows the energy levels for a single hole, the theory of reference 1 can be applied, the interaction energy between the two neutron holes being given by the same formulas as for two identical nucleons. For the purpose of calculating the energy levels, two holes in a closed shell behave in exactly the same way as two two nucleons outside a closed shell (this point was not clearly expressed in reference 1). The necessary starting point is furnished by the levels of  $Pb^{207}$ , which are the

TABLE VIII. Energy levels of  $Pb^{207}$ .

Level	Parity	Energy (MeV)
$p_{1/2}$	—	0.00
$f_{5/2}$	—	0.570
$p_{3/2}$	—	0.87
$i_{13/2}$	+	1.634
$h_{9/2}$	—	2.35

<sup>21</sup> Rose, Goertzel, Spinrad, Harr, and Strong, Phys. Rev. **83**, 79 (1951).

levels of a single hole. Since the publication of the earlier work<sup>1</sup> better information on the levels of  $Pb^{207}$  has been accumulated,<sup>15,17,22,23</sup> and we adopt the levels given in Table VIII. The present scheme differs from the older one by the disappearance of the  $f_{7/2}$  level from 1.11 MeV and of the four levels above 2 MeV, which are not confirmed by the recent work. The  $f_{7/2}$  level is probably somewhere close above 2.35 MeV, but there is no information concerning its position at present. The levels of  $Pb^{206}$  are derived by assigning one of the levels of Table VIII to each neutron hole. From each such pair of  $Pb^{207}$  levels (configuration) a number of energy levels of different spins can be constructed for  $Pb^{206}$ , according to the ordinary rules of vector coupling. As an example, the configuration  $p_{1/2}f_{5/2}$  contains two levels (2+ and 3+). If there were no interaction between the holes the energy of the levels would be just the sum of the energies of the two  $Pb^{207}$  levels in the configuration, and all  $Pb^{206}$  levels from the same configuration would be degenerate, but because of the interaction the levels are split. According to the simplified form of the theory,<sup>1</sup> which assumes that the range of the nuclear forces is negligible compared with the diameter of the nucleus, some levels are not shifted at all, while others are depressed. The energy of the unshifted levels of a configuration will be called its "head;" referred to a nominal zero it is the sum of a pair of values from Table VIII.

The ground state of  $Pb^{206}$  corresponds to both holes being in the  $p_{1/2}$  level, i.e., the configuration  $p_{1/2}^2$ . Because of the exclusion principle, there is only the state  $I=0(+)$  in this configuration. Interaction depresses its energy below the nominal zero by an amount which we estimate, for reasons given later, to be 0.77 MeV. The head of a configuration, referred to the ground state of  $Pb^{206}$  as zero, is therefore obtained by adding 0.77 MeV to the sum of the two  $Pb^{207}$  energies. Table IX lists the lowest thirteen configurations, their

TABLE IX.  $Pb^{206}$  configurations.

	Config-uration	Head (MeV)	Spins	Parity	Approx-imate inter-action parameter (MeV)
1	$p_{1/2}^2$	(0.77)	0	+	0.4
2	$p_{1/2}f_{5/2}$	1.34	2,3	+	0.3
3	$p_{1/2}p_{3/2}$	1.64	1,2	+	0.4
4	$f_{5/2}^2$	1.91	0,2,4	+	0.4
5	$f_{5/2}p_{3/2}$	2.21	1,2,3,4	+	0.3
6	$p_{1/2}i_{13/2}$	2.40	6,7	—	0.2
7	$p_{3/2}^2$	2.51	0,2	+	0.4
8	$f_{5/2}i_{13/2}$	2.97	4,5,6,7,8,9	—	0.2
9	$p_{1/2}h_{9/2}$	3.12	4,5	+	0.2
10	$p_{3/2}i_{13/2}$	3.27	5,6,7,8	—	0.2
11	$f_{5/2}h_{9/2}$	3.69	2,3,4,5,6,7	+	0.2
12	$p_{3/2}h_{9/2}$	3.99	3,4,5,6	+	0.2
13	$i_{13/2}^2$	4.04	0,2,4,6,8,10,12	+	0.5

<sup>22</sup> D. E. Alburger (unpublished).

<sup>23</sup> J. R. Prescott, Proc. Phys. Soc. (London) **67**, 540 (1954).

heads, the spins of the levels derived from them, and their parities. It should be noticed that if both holes occupy the same  $Pb^{207}$  level, only even values of  $I$  are allowed by the exclusion principle.

The amount by which the levels are depressed by the interaction between the holes is expressible in terms of a positive parameter  $\epsilon$  (called  $-\epsilon_s$  in reference 1) involving the strength of the singlet nuclear force and an integral over the radial wave functions of the single neutron levels. There is a different  $\epsilon$  for each configuration, whose value can be calculated if one knows the wave functions. As the theory is at best approximate and is only used here as a guide, no attempt has been made at performing the calculation. Instead, rough values of  $\epsilon$  have been estimated semi-empirically and are listed in Table IX.

In this way the theory can be used to predict the pattern of the energy levels of  $Pb^{206}$ . In Table X the energies of all levels up to about 3.7 Mev, expressed in terms of the parameters  $\epsilon_1, \dots, \epsilon_{13}$ , are arranged according to their spin and parity. It will be seen that except for the  $0+$  levels the coefficients of  $\epsilon$  are not large, so that, with these exceptions, errors in estimating  $\epsilon$  do not matter much.

When two levels of the same spin and parity are predicted to be close together the theory breaks down because configuration interaction becomes important. This is most likely to be a large effect for the  $0+$  levels, for which the matrix elements of configuration coupling are the largest, and for that reason, and the large coefficient of  $\epsilon$ , their predicted position is liable to be in error by as much as 1 Mev. This large uncertainty in the  $0+$  levels is indicated in Table X by  $\sim$ . Other levels are probably reliable to 0.3 Mev or better if the coefficient of  $\epsilon$  is less than 1 and no perturbing level is close.

In addition to these levels one must expect the presence of core excitation levels. Information on these may be obtained from the known excited levels of

$Pb^{208}$ . The first two are at 2.615 Mev ( $I=3-$ ) and 3.198 Mev ( $I=5-$ ).<sup>24</sup> Since they are not excited<sup>5</sup> in the reaction  $Pb^{207}(d,p)Pb^{208}$ , they presumably arise from an excited proton, the neutrons remaining effectively undisturbed. Similar levels at about the same energy may therefore be expected in  $Pb^{206}$ , and have been listed, marked with an  $a$  in Table X. More complex excited proton levels, in which the neutrons are also disturbed from the  $p_{1/2}^{-2}$  configuration, must also be expected to start at around  $2.6+0.803=3.4$  Mev. Many spins are possible, with odd parity, but these levels are not listed, although they may well fall into the interesting energy range. According to Harvey<sup>4</sup> the lowest neutron excitation level in  $Pb^{208}$  is at 3.37 Mev. Since it probably corresponds to a neutron promoted from the  $p_{1/2}$  level to the  $2g_{9/2}$  level, in  $Pb^{206}$  the corresponding level will arise from the promotion of an  $f_{5/2}$  neutron, the  $p_{1/2}$  level being empty in the ground state, and so will be roughly 0.57 Mev higher (i.e., at 3.9 Mev). This is outside the present range of interest.

This information is illustrated in Fig. 8, which combines the experimental data and the shell model predictions in the form of a Grottrian diagram. Predicted levels which do not correspond to an observed level have been marked by broken lines, while observed levels are shown as full lines. Comparison of Fig. 8 with Table X shows that the experimental levels can be identified with predicted levels in a natural manner.

Inspection of Table X at once shows some of the characteristic features of the term diagram of  $Pb^{206}$  which proved useful in the interpretation of the spectrum. Particularly important is the prediction that the lowest level of spin  $I=7$  is lower than any levels of spin  $I=5, 6$ , and  $\geq 8$ . If this level is reached, therefore, it will de-excite by an  $E3$  transition to a  $4+$  level, followed by a cascade via  $3+$  and  $2+$  levels to the  $0+$  ground state. When the 516.1-kev  $E3$  transition was found experimentally, its place in the scheme could immediately be understood and be used firmly to anchor the other levels.

We now return to the reasons for taking 0.77 Mev for the shift of the ground state relative to the nominal zero. Having once obtained a reasonable identification of the observed levels, it was seen that two of them were levels in which the approximate theory predicts no shift from the configuration head, so that their position relative to the nominal zero is known. These are the  $p_{1/2}f_{5/2}$   $3+$  level at 0.57 Mev from the nominal zero, actually at 1.340 Mev, whence the shift is  $1.34 - 0.57 = 0.77$  Mev, and the  $p_{1/2}i_{13/2}$   $6-$  level at 1.635 Mev from the nominal zero, actually at 2.385 Mev, whence the shift is calculated to be  $2.385 - 1.635 = 0.75$  Mev. The agreement between these two values is better than could have been expected. The value 0.77 Mev was adopted because the  $3+$  level is less likely to

TABLE X. Predicted levels of  $Pb^{206}$ .

Spin and parity	Predicted energies (Mev) (neglecting configuration interaction)
$0+$	$\sim 0.77 - \epsilon_1 = 0.00, \sim 1.91 - 3\epsilon_4, \sim 2.51 - 2\epsilon_7, \sim 4.04 - 7\epsilon_{13}, \dots$
$1+$	1.64, 2.21, $\dots$
$2+$	$1.34 - 1.2\epsilon_1, 1.64 - 0.8\epsilon_3, 1.91 - 0.7\epsilon_4, 2.21 - 0.35\epsilon_6, 2.51 - 0.4\epsilon_7, 3.69 - 2.9\epsilon_{11}, \dots$
$3+$	1.34, 2.21, 3.69, $\dots$
$3-$	2.6, <sup>a</sup> $\dots$
$4+$	$1.91 - 0.3\epsilon_4, 2.21 - 1.1\epsilon_6, 3.12 - 1.1\epsilon_9, 3.69 - 1.0\epsilon_{11}, \dots$
$4-$	2.97, $\dots$
$5+$	3.12, 3.69, $\dots$
$5-$	$2.97 - 0.3\epsilon_8, 3.27 - 1.8\epsilon_{10}, 3.2^a, \dots$
$6+$	$3.69 - 0.5\epsilon_{11}, \dots$
$6-$	2.40, 2.97, 3.29, $\dots$
$7+$	3.69, $\dots$
$7-$	$2.40 - 0.9\epsilon_6, 2.97 - 0.6\epsilon_8, 3.27 - 0.6\epsilon_{10}, \dots$
$8-$	2.97, 3.27, $\dots$
$9-$	$2.97 - 1.6\epsilon_8, \dots$

<sup>a</sup> Proton excitation levels.

<sup>24</sup> Elliott, Graham, Walker, and Wolfson, Phys. Rev. **93**, 356 (1954).



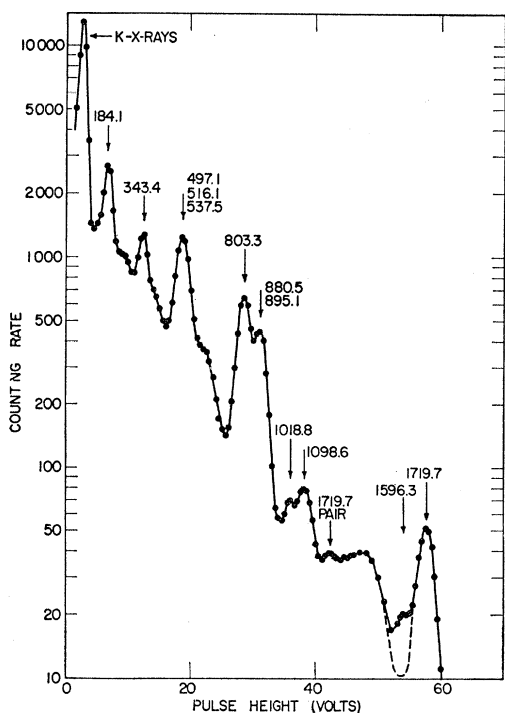


Fig. 9. Differential pulse-height spectrum of  $\text{Bi}^{206}$  gamma rays in a NaI scintillation spectrometer.

there definite evidence for a very pure  $M1$ . From photographic exposures made in a semicircular beta spectrograph, Michelich has found<sup>26</sup> no detectable  $L_{III}$  line in the 184.1-keV transition and thus has shown that there is at most a fraction of a percent of  $E2$  present. If no allowance is made for mixtures, the transition intensities derived from the  $K$ -conversion line data and the theoretical conversion coefficients form a reasonably consistent scheme except for the intensity of the 537.5-keV gamma which comes out too low for proper balancing. The assumption that the 537.5-keV transition contains  $M1+E2$  in the ratio of 5 to 3 will account correctly for the balance. As the admixture might, on general grounds, be expected to increase progressively with increasing energy the intensities calculated for the  $M1(+E2)$  transitions have, rather arbitrarily, been increased by a factor of from 20 to 50 percent in column 5 of Table XI.

According to the analysis the primary excitation is shared about equally between the two top 5- levels. There is no direct evidence of other levels being appreciably excited although weak excitation of the doubtful 3124.7-keV level is suggested.

Relative intensities of conversion lines corresponding to the 516.1 and 202.5 keV  $E3$  isomeric transitions have already been published,<sup>5</sup> but unfortunately the necessary counter window corrections to the 202.5 lines had been overlooked. The corrected ratio of the two  $E3$   $K$ -line intensities, as derived from Table XI, leads to a

revised ratio of unconverted gammas of  $\sim 760$ , in good agreement with that expected from the seventh power of their energy ratio. This correction also changes the ratio of 516.1 to 202.5-keV transition probabilities to 120, from which the partial half-life of the 202.5-keV transition is found to be  $\sim 0.02$  sec.

In order to check some of the intensities and thereby give further supporting evidence for the decay scheme of  $\text{Bi}^{206}$ , a sodium iodide scintillation spectrometer was used to examine the gamma spectrum. The detector was a sealed Harshaw unit containing a crystal 3.8 cm in diameter and 2.5 cm high. This had been mounted on a Dumont 6292 photomultiplier and set into operation at Brookhaven by Dr. B. J. Toppel. With  $\text{Cs}^{137}$  a resolution of 7.5 was observed.

A source of  $\text{Bi}^{206}$  was prepared by bombarding lead in the Brookhaven cyclotron using deuterons reduced by an aluminum absorber from the full 22-MeV beam energy to about 16 MeV. According to the findings discussed in Sec. II any background of  $\text{Bi}^{205}$  was thereby avoided. Chemical separation of the bismuth was performed in the usual way and a small amount of the activity was placed above the NaI crystal.

Figure 9 shows the differential pulse height spectrum using a channel width of 0.8 volt. The peaks are identified with  $\text{Bi}^{206}$  gamma energies from Table I.

Relative gamma-ray intensities were found by determining the number of electrons in each photopeak and correcting for the efficiency of the crystal. The

TABLE XI. Transitions and intensities in the decay of  $\text{Bi}^{206}$ .

Gamma	Energy (keV)	Multipole	$K$ -line intensity (electrons per 100 disintegrations)	Transition intensity adopted from $K$ -line intensities (803.3=100)	Transition intensity from gamma meas.
1	184.1	$M1$	28	40	45
2	234.3	$M1$	0.24	0.6	
3	262.8	$M1$	2.1	6.1	
4	343.4	$M1$	6.6	30	25
5	386.0	$M1$	0.13	0.6	
6	398.1	$M1(+E2)$	1.76	12	
7	497.1	$M1(+E2)$	1.37	15	
8	516.1	$E3$	1.95	41	76
9	537.5	$M1(+E2)$	2.08	32	
10	620.6	$M1(+E2)$	0.27	6	
11	632.2	$M1(+E2)$	0.21	4	
12	657.3	$M1(+E2)$	0.084	2	
13	803.3	$E2$	0.85	100	100
14	880.5	$E2$	0.48	68	
15	895.1	$M1(+E2)$	0.32	17	65
16	1018.8	$M1(+E2)$	0.11	8	8
17	1098.6	$E1$	0.029	16	14
18	1596.3	$E1$	0.0054	6	5.5
19	1719.7	$E1$	0.029	34	32
20	123.6	$M1$	0.069	0.1	
21	202.5	$E3$	0.020	0.35	
22	313.6	$M1$	0.14	0.5	
23	739.9	$E1$	0.011	3	
24	753.9	$E2$	0.0074	2	
25	816.3	$M1(+E2)$	0.0025	0.1	
26	841.7	$E1$	0.0050	2	
27	1405.2	$E1$	0.0020	2	
28	107.2	$E1$	0.23	0.2	

<sup>26</sup> J. W. Michelich (private communication).

photoline intensities were measured using a nonoverload amplifier and a differential pulse-height analyzer, each photoline being run after adjusting the voltage on the photomultiplier so that the peak was centered at a pulse height of 35 volts. After subtraction of an estimated background the areas under the curves were measured with a planimeter.

The total detection efficiency *versus* energy for this size crystal has been calculated<sup>27</sup> by McGowan, while Heath, Bell, and Davis have measured<sup>28</sup> the ratio of the full energy loss peak to total intensity at a number of energies. By combining these data a curve of photopeak efficiency *versus* energy was derived. As expected, this was found to fall off a little faster with energy than the curve published<sup>29</sup> by Hornyak and Coor for a slightly larger crystal (4-cm diam by 3 cm high). Using this curve, extrapolated in the case of the 184.1-keV gamma, the line intensities were converted to gamma intensities and finally the transition intensities were obtained after correcting for internal conversion based on the multipole orders given in column 3 of Table XI. This correction was large only for the 184.1 and 343.4-keV transitions. The resulting transition intensities are given in the last column of Table XI. Within the estimated errors of approximately 30 percent, it is seen that the directly measured intensities of gamma rays accessible to the experiment are in agreement with those derived from the conversion line intensities. These data give strong support to a number of the spin and parity assignments which were made at first mostly on the basis of the theoretical analysis.

$K/L$  ratios, plotted against  $Z^2/E$  in Fig. 10, were taken from the double-focusing spectrometer measurements described in Sec. II except for the 184.1-keV transition whose low energy made it more desirable to use the earlier lens spectrometer data where the window corrections were smaller. Peak heights were used as a measure of line intensity in all cases. An inspection of Fig. 2 shows that the  $L_{III}$  line of the 516.1-keV transition is almost resolved so that its contribution to the  $L_{I+II}$  peak height is not appreciable. Thus the

TABLE XII. Conversion electrons and unconverted gamma rays per 100  $Bi^{206}$  disintegrations of the two  $E3$  isomeric transitions in  $Pb^{206}$ —experimental and theoretical  $K/L_{I+II}$  ratios.

$E_\gamma$ (keV)	Esti- mated uncon- verted $\gamma$ 's	$K$	$L_{I+II}$	$L_{III}$	$M$	$N$	$K/L_{I+II}$ (theo- retical)
202.5	0.05	0.020	0.10	0.044	0.039	...	0.20 0.192 <sup>a</sup>
516.1	38	1.95	1.09	~0.2	0.36	~0.07	1.78 1.58 <sup>b</sup>

<sup>a</sup> Calculated for  $k=0.4$   $mc^2=205$  keV.

<sup>b</sup> Calculated for  $k=1.0$   $mc^2=511$  keV.

<sup>27</sup> F. K. McGowan (privately circulated tables). See Phys. Rev. 93, 163 (1954).

<sup>28</sup> Heath, Bell, and Davis, Oak Ridge National Laboratory Report ORNL 1415 (unpublished).

<sup>29</sup> W. F. Hornyak and T. Coor, Phys. Rev. 92, 675 (1953).

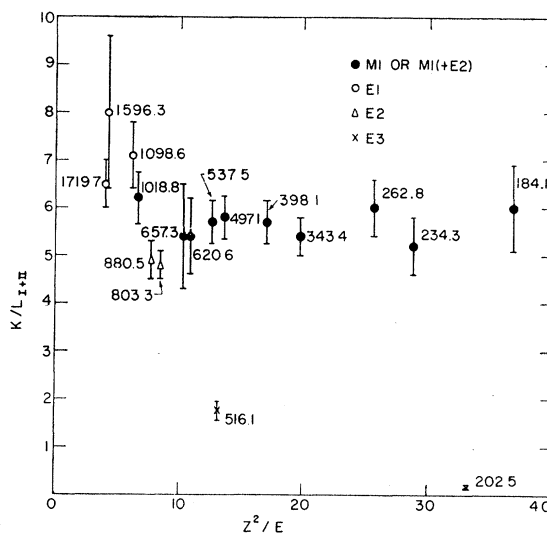


FIG. 10.  $K/L_{I+II}$  conversion ratios for  $Pb^{206}$  transitions.

$K/L$  ratios in Fig. 10 represent  $K/L_{I+II}$  with the possible exception of higher energy lines where the  $L_{III}$  line is relatively closer to the  $L_{I+II}$  peak.

Many of these  $K/L$  ratios may be compared directly with theoretical values derived from the  $K$ -conversion coefficients already published<sup>21</sup> together with some  $L$ -conversion coefficients which have been privately distributed by Dr. M. E. Rose. Because the present set of  $L$ -conversion coefficients covers only a few values of  $Z$  it is not yet possible to interpolate for  $Z=82$ . Ratios have therefore been computed for  $Z=85$  and it has been assumed that the ratios for  $Z=82$  are not appreciably different. Although no  $L_{III}$  conversion coefficients are available as yet the lack of these is not serious in most cases owing to the probability that  $L_{III}$  lines did not contribute to the experimental ratios because of the high resolution used.

Table XII gives the experimental conversion line intensities of the two  $E3$  isomeric transitions which have now been changed from the previously published values<sup>5</sup> so as to take counter window absorption into account. The last two columns indicate that the agreement between the experimental and theoretical  $K/L_{I+II}$  values is very good. For the 202.5-keV transition an extrapolation of the  $K$ -conversion  $E3$  curve<sup>21</sup> was necessary in order to derive  $K/L_{I+II}$ .

Theoretical  $K/L_{I+II}$  ratios ( $Z=85$ ) for a number of  $E1$ ,  $M1$ , and  $E2$  transitions in  $Pb^{206}$  may also be compared with Fig. 10. The calculations show that  $M1$ 's above  $Z^2/E=6$  have a very nearly constant  $K/L_{I+II}$  ratio of about 5.9. According to Fig. 10 none of the  $M1$  or  $M1(+E2)$  transitions assigned in the scheme have ratios deviating from this value by more than the experimental error. The two  $E2$  transitions of 803.3 and 880.5 keV have  $K/L_{I+II}$  ratios whose positions are consistent with a value of 4.55 calculated for a gamma of



770 keV ( $1.5 mc^2$ ,  $Z^2/E=8.8$ ). Two other experimental  $\text{Bi}^{206}$   $K/L$  ratios which one may compare with theory are the 1098.6 keV  $E1$  and the 1018.8 keV  $M1$  whose calculated  $K/L_{I+II}$  ratios should be 6.8 and 5.9, respectively. Again the measurements are in agreement, but because of the errors one cannot distinguish between  $E1$ 's and  $M1$ 's in this region of low  $Z^2/E$  using these data alone.

Thus in every case for which comparison can be made the agreement between the experimental and theoretical  $K/L$  ratios is excellent. Had the theoretical values been available earlier the initial analysis of the  $\text{Pb}^{206}$  scheme would have been aided considerably. For example the  $K/L_{I+II}$  ratios computed at  $k=1.0=511$  keV, or close to the 516.1-keV isomeric transition, vary from 5.8 down to 2.1 for magnetic radiation ranging from  $M1$  to  $M5$ , while for the electric multipoles an  $E2$  would have a ratio of 3.4 and an  $E4$  a ratio of 0.86. The assignment of the 516.1-keV gamma ray as  $E3$  on the basis of the measured  $K/L_{I+II}$  ratio of 1.78 is unambiguous and gives another independent check on this transition.

## XII. DISCUSSION

The agreement between the observed levels of  $\text{Pb}^{206}$  and the predictions of the shell model can be considered very satisfactory. The shell model can also be used to understand the nature and spin of the main capturing states, which, by fixing the starting point of the gamma-ray cascade, also contribute to the characteristic features of the  $\text{Bi}^{206}$  spectrum.

One first needs to estimate the spin of the ground state of  $\text{Bi}^{206}$ . This is a nucleus with one proton outside the closed shell and three holes in the closed neutron shell. We assume that the proton is in the  $h_{9/2}$  level, by analogy with stable  $\text{Bi}^{209}$ , and that the neutron configuration is  $p_{1/2}^{-2}f_{5/2}^{-1}$ , i.e., an  $f_{5/2}$  hole in a closed subshell. By a theorem due to Kurath,<sup>30</sup> the lowest state of a configuration with one proton in a level  $j$  and one neutron hole in a level  $j'$  is the one with  $I=j+j'-1$ , which in the present case is  $9/2+5/2-1=6$ . The parity is even. If this is true, electron capture will go preferentially to states of spin  $I=5, 6, 7$  in  $\text{Pb}^{206}$ , if they are energetically accessible, these transitions being either allowed or first forbidden according to parity. Since in such a heavy nucleus first forbidden transitions which are not  $l$  forbidden are nearly as probable as allowed transitions, the parity is not very important. Capture to other spin states may be expected to be more highly forbidden.

The degree of forbiddenness is not the only relevant factor in capture, however, for if the shell model is a good approximation the nuclear matrix element for the capture in any of the two-hole levels of  $\text{Pb}^{206}$  must be very small, since such a transition involves not only a change of a proton into a neutron, but also a further neutron jump. The only exceptions to this limitation are

the highly forbidden transitions in which the  $h_{9/2}$  proton changes into a neutron in one of the available  $p_{1/2}$  or  $f_{5/2}$  states (i.e.,  $I=6 \rightarrow I=0, 2, \text{ or } 3$ ), or the energetically inaccessible states in which the newly formed neutron is in the next shell. This indicates that if a suitable proton excitation level of  $\text{Pb}^{206}$  is available this will be the main capture level. Such a level is furnished by the predicted 5- level at about 3.2 MeV, which is plausibly a mixture of the proton configurations  $h_{9/2}5_{1/2}^{-1}$  and  $h_{9/2}d_{3/2}^{-1}$ , coupled to the ground neutron configuration  $p_{1/2}^{-2}$ . Electron capture can then take place with the conversion of a  $d_{3/2}$  proton (from inside the 82-shell) in  $\text{Bi}^{206}$  into an  $f_{5/2}$  neutron, filling that level in forming  $\text{Pb}^{206}$ . This satisfactorily explains why the main capture is observed to two 5- levels of high excitation (3.4035 and 3.2801 MeV). That there are two such levels, instead of one, can plausibly be explained either by the presence of the  $p_{3/2}i_{13/2}$  5- level very close to the proton excited level, so that the two levels perturb each other and share their characteristics, or be ascribed to one of the more complex proton excitation levels discussed in Sec. X. That this is essentially the mechanism of capture is supported by the short half-life of  $\text{Bi}^{206}$  (6.4 days), compared with the long half-life (50 years) of  $\text{Bi}^{207}$ , for which no excited proton level in  $\text{Pb}^{207}$  is available.

That capture takes place mainly into two highly excited 5- levels at once explains the unusual complexity of the spectrum. The main de-excitation of the capture levels occurs by  $E1$  transitions to the 4+ level at 1683.8 keV, and by  $M1$  transitions to the 2782.9 5- and the two 6- levels at 3017.1 and 2384.8 keV. Cascades through the odd levels lead either to the lower 6- level, and thence in two steps via the isomeric level to the lowest 4+ level, or else more directly to the 4+ level. After that, the nucleus cascades through the 1340.8 and 803.3 keV levels to ground. Other levels are only weakly excited. Since at each step the most probable transition tends to be the one involving the greatest energy with the least spin change, one readily understands why no 1+, and only the lowest 0+, 2+ and 3+ levels have been detected, and also why no 8-, 9- or higher 7- levels have been found.

A point which may be mentioned is that although the first excited level is 2+ as in most even-even nuclei, the explanation is here different. Usually the first excited state belongs to the same configuration as the ground state, while in  $\text{Pb}^{206}$  the ground configuration,  $p_{1/2}^2$ , contains only the one state 0+, and the first excited state belongs to  $p_{1/2}f_{5/2}$ . This serves to explain its unusually high energy for such a heavy nucleus.

In one way the outcome of the present investigation is disappointing. It had been hoped that by a study of the  $\text{Bi}^{206}$  spectrum one could gain enough information concerning all the levels of several configurations to put the theory to a quantitative test, and to learn something concerning the importance of configuration interaction. Unfortunately not more than two levels belonging to

<sup>30</sup> D. Kurath, Phys. Rev. **87**, 528 (1952).

any one configuration have been observed, which is not enough to test the theory. This lack of information arises because the higher states of low spin are not reached by the gamma cascade. A more searching test of the theory must await the investigation of the low-spin levels of  $Pb^{206}$  by other means, such as  $(d,t)$  reactions employing improved resolution or excitation by inelastic scattering of neutrons.

The correlation between the  $Pb^{206}$  levels found in the decay of  $Bi^{206}$  and the levels found by Harvey<sup>4</sup> in the reaction  $Pb^{207}(d,t)Pb^{206}$  is interesting. This is essentially a neutron pick-up reaction, and since in the ground state of  $Pb^{207}$  there is already a hole in the  $p_{1/2}$  level, it is to be expected that those levels of  $Pb^{206}$  which are strongly excited are those with a  $p_{1/2}$  hole. These are (i) the ground state (ii) the 2+ and 3+ states of  $p_{1/2}f_{5/2}$  (803.3 and 1340.8 keV), (iii) the 1+ and 2+ states of  $p_{1/2}p_{3/2}$  (not found in the present work, but predicted near 1.64 and 1.35 MeV, respectively), (iv) the 6- and 7- states of  $p_{1/2}i_{13/2}$  (2384.8 and 2200.3 keV), and (v) the 4+ (predicted near 2.9 MeV) and 5+ (3124.7 keV?) levels of  $p_{1/2}h_{9/2}$ . In addition, because of strong configuration interaction in 0+ states, one might expect to find the next 0+ level (1 MeV?). The observed triton group indicating a level at 0.86 MeV can correspond to 803.3 keV unresolved from the 0+ level; that at 1.37 MeV the 1340.8 keV level unresolved from the second 2+ level; 1.71 MeV the 1+ level; 2.22 MeV the unresolved 6- and 7- levels; and 3.03 the unresolved  $p_{1/2}h_{9/2}$  doublet. Better agreement can hardly be expected, for the triton groups are 300 keV wide and curve fitting was necessary to resolve them into the above groups.<sup>4</sup> Better resolution would certainly be rewarding.

Although the shell model appears to give reliable predictions concerning the energies of the levels and the selection rules for electron capture, it is unreliable about radiation intensities. In its crudest form it would predict very small transition probabilities for electric multipoles between any of the neutron levels, which is quite inconsistent with the observed speed of the  $E3$  isomeric transitions. According to the Weisskopf formula<sup>31</sup> the lifetime for a 516-keV  $E3$  proton transition is 13 microseconds, while the observed lifetime (145 microseconds) is only 11 times slower. Such speed for what is essentially a neutron transition cannot be explained by any simple configuration mixing and must be taken as indicating some kind of collective motion

in which either the neutrons "convect" electric charge, or the nucleus as a whole is deformed as in the collective model.<sup>32</sup> The strong 880.5-keV  $E2$  crossover, and the necessity of assuming  $M1+E2$  for the 537.5 line to balance the intensities in Table XI also point in a similar direction.

The energy release in the disintegration of  $Bi^{206}$  can be estimated to lie between 3.4 and 3.7 MeV from the fact that the 3403.5-keV level is strongly excited, while no measurable excitation of any higher level takes place. The absence of positrons is easily understood. Although there is enough energy (>181 keV) for positron emission to the 7- state at 2200.3 keV, the calculated ratio of positrons to  $K$  captures<sup>33</sup> for a positron energy less than 300 keV is less than 1 in  $10^4$ . As the number of  $K$  captures into this state can be estimated from the gamma-ray intensities at not more than about ten percent per disintegration the positron yield cannot much exceed 1 in  $10^6$ . Transitions to energetically more favored states are at least second forbidden and cannot be expected to contribute appreciably to the positron yield.

### XIII. ACKNOWLEDGMENTS

The authors would like to thank Professor Manne Siegbahn for making the facilities of the Nobel Institute of Physics available for the major part of the experimental work and Professor Kai Siegbahn for the use of equipment at the Royal Institute of Technology. Their kind hospitality to the first-named author during 1952-1953 is greatly appreciated. Experiments at the Nobel Institute were made possible by the generous assistance of a number of persons. Dr. H. Atterling and the crew of the large cyclotron carried out many target irradiations essential to this project. Dr. L. Melander arranged for the chemical separations, which were performed by Dr. W. Forsling and Mr. T. Karlsson of his group. Thanks are also due Mr. B. Åström who gave considerable assistance with various electronic equipments and scintillation detectors. Experiments at the Royal Institute of Technology were aided by the help of Dr. T. Gerholm and other members of Professor Kai Siegbahn's group. Professor H. Slätis and Dr. A. Hedgran gave much of their time in discussing the use of the double-focusing and intermediate-image spectrometers. The authors are also indebted to the crew of the Brookhaven cyclotron for bombardments and to Mrs. Elizabeth Wilson Baker for chemical separations.

<sup>31</sup> J. M. Blatt and V. F. Weisskopf, *Theoretical Nuclear Physics* (John Wiley and Sons Inc., New York, 1952), p. 627.

<sup>32</sup> A. Bohr, Kgl. Danske Videnskab. Selskab, Mat.-fys. Medd 26, No. 14, (1952).

<sup>33</sup> E. Feenberg and G. Trigg, Revs. Modern Phys. 22, 399 (1950).